

## First-principles calculation of the superconducting transition in MgB<sub>2</sub> within the anisotropic Eliashberg formalism

Hyoung Joon Choi,<sup>1</sup> David Roundy,<sup>1,2</sup> Hong Sun,<sup>1</sup> Marvin L. Cohen,<sup>1,2</sup> and Steven G. Louie<sup>1,2</sup>

<sup>1</sup>Department of Physics, University of California at Berkeley, Berkeley, California 94720

<sup>2</sup>Materials Sciences Division, Lawrence Berkeley National Laboratory, Berkeley, California 94720

(Received 11 June 2002; published 30 July 2002)

We present a study of the superconducting transition in MgB<sub>2</sub> using the *ab initio* pseudopotential density-functional method, a fully anisotropic Eliashberg equation, and a conventional estimate for  $\mu^*$ . Our study shows that the anisotropic Eliashberg equation, constructed with *ab initio* calculated momentum-dependent electron-phonon interaction and anharmonic phonon frequencies, yields an average electron-phonon coupling constant  $\lambda=0.61$ , a transition temperature  $T_c=39$  K, and a boron isotope-effect exponent  $\alpha_B=0.32$ . The calculated values for  $T_c$ ,  $\lambda$ , and  $\alpha_B$  are in excellent agreement with transport, specific-heat, and isotope-effect measurements, respectively. The individual values of the electron-phonon coupling  $\lambda(\vec{k},\vec{k}')$  on the various pieces of the Fermi surface, however, vary from 0.1 to 2.5. The observed  $T_c$  is a result of both the raising effect of anisotropy in the electron-phonon couplings and the lowering effect of anharmonicity in the relevant phonon modes.

DOI: 10.1103/PhysRevB.66.020513

PACS number(s): 74.25.Kc, 63.20.Ry, 74.20.-z

Although MgB<sub>2</sub> is a readily available *sp*-bonded material, superconductivity in this material with a transition temperature of  $T_c=39$  K was found only very recently.<sup>1</sup> This relatively high  $T_c$  has motivated many studies, as has the observation that the detailed superconducting properties of MgB<sub>2</sub> show significant deviations from those calculated using the standard BCS model. The isotope-effect exponent for boron  $\alpha_B$  is reduced substantially from the conventional value for *sp* metals,<sup>2,3</sup> and the average electron-phonon coupling strength  $\lambda$  obtained from specific-heat measurement<sup>4-7</sup> seems too small to justify the high  $T_c$ . In addition, specific-heat measurements,<sup>4-7</sup> tunneling<sup>8</sup> and photoemission<sup>9</sup> spectra, and point-contact spectroscopy<sup>10,11</sup> show low-energy excitations suggesting a secondary gap. Theoretical calculations show that the Fermi surface has several pieces and is very anisotropic,<sup>12</sup> and that the electron-phonon coupling is dominated by the in-plane B–B stretching modes ( $E_{2g}$ ),<sup>12-14</sup> which have a large anharmonicity.<sup>15,16</sup> The electron-phonon interaction varies strongly on the Fermi surface,<sup>16,17</sup> and a two-band model suggests a multigap scenario.<sup>16,18</sup> However, there has not yet been a quantitative, first-principles calculation of  $T_c$  including the full variation of the electron-phonon interaction on the Fermi surface and the anharmonicity of the phonons to help confirm the phonon-mediating pairing mechanism for superconductivity in MgB<sub>2</sub>.

In this Communication, we present  $T_c$  and isotope-effect exponents for MgB<sub>2</sub> obtained by solving the  $\vec{k}$ - and  $\omega$ -dependent Eliashberg equation. It is shown that the anisotropy (i.e., the electronic-state dependence) of the electron-phonon interaction on the Fermi surface is strong enough to raise  $T_c$  to 39 K even though the interaction is weakened by the anharmonicity of the phonons as compared to the harmonic case. In addition, it is shown that the anharmonicity of the phonons reduces  $\alpha_B$  to 0.32. These results show that conventional phonon-mediated electron pairing theory can explain superconductivity in MgB<sub>2</sub> when both the anisotropy

of the electron-phonon interaction and the anharmonicity of the phonons are properly taken into account. The solution of the full Eliashberg equation at low  $T$  further yields different gap values for the different parts of the Fermi surface. The gap value distribution clusters into two groups—a small value of  $\sim 2$  meV and a large value of  $\sim 7$  meV. This feature and its physical consequences will be described in more detail in a future publication.<sup>19</sup>

The phonon frequencies and electron-phonon matrix elements are calculated using *ab initio* pseudopotentials and the local-density approximation. We used a  $12\times 12\times 12$   $k$ -point grid in the Brillouin zone (BZ) for self-consistent calculations and a  $18\times 18\times 12$  grid for the Fermi surface properties, and included plane waves up to 60 Ry as a basis to expand the electronic wave functions. The calculated equilibrium lattice constants are  $a=3.071$  Å and  $c=3.578$  Å, in good agreement with measured values.<sup>1</sup> We performed total-energy calculations with frozen phonons for all phonon modes at all the high-symmetry points of the BZ. The variation of the total energy with a frozen phonon amplitude is fitted with a fourth-order polynomial to account for the phonon anharmonicity. To obtain the harmonic phonon frequency, we use the quadratic term of the fitted curve and calculate the frequency classically, whereas for the anharmonic phonon frequency, we calculate quantum-mechanical vibrational states including the anharmonic terms, and take the energy difference of the two lowest states. In the case of the degenerate, in-plane B–B stretching modes ( $E_{2g}$ ) at  $\Gamma$  and A, we calculate quantum-mechanical vibrational states in two dimensions after the total energy is fitted in a plane with  $E(r,\theta)=E_0+c_2r^2+c_4r^4+(c_3r^3+c_5r^5)\cos(3\theta)$ . We use natural atomic weights for B and Mg, that is, 10.81 for B and 24.31 for Mg, but <sup>10</sup>B or <sup>26</sup>Mg are used when we recalculate the phonon frequency for the isotope effect. The linear electron-phonon matrix elements are evaluated directly from the total self-consistent change in the crystal potential caused by a frozen phonon.

Table I shows the frequency of the in-plane B–B stretching mode ( $E_{2g}$ ) at  $\Gamma$ . This mode is doubly degenerate along

TABLE I. Transition temperature  $T_c$  and isotope-effect exponents  $\alpha$  with  $\mu^*(\omega_c)=0.12$ . Numbers in parentheses are the values of  $\alpha_B$  when  $\delta\mu^*(\omega_c)$  of Eq. (3) is ignored. The averaged electron-phonon coupling  $\lambda$  and the frequency  $\omega_{ph}$  of the in-plane B–B stretching modes ( $E_{2g}$ ) at  $\Gamma$  are also included.

	Harmonic		Anharmonic		Experiment
	Isotropic	Anisotropic	Isotropic	Anisotropic	
$T_c$	28 K	55 K	19 K	39 K	39 K <sup>a</sup>
$\alpha_B$	0.42 (0.46)	0.46 (0.48)	0.25 (0.27)	0.32 (0.33)	0.26 <sup>b</sup> , 0.30 <sup>c</sup>
$\alpha_{Mg}$	0.04	0.02	0.05	0.03	0.02 <sup>c</sup>
$\lambda$	0.73		0.61		0.58 <sup>d</sup> , 0.62 <sup>e</sup>
$\omega_{ph}$	62.7 meV		75.9 meV		75.9 <sup>f</sup> , 76.9 <sup>g</sup>

<sup>a</sup>Reference 1.

<sup>b</sup>Reference 2.

<sup>c</sup>Reference 3.

<sup>d</sup>Reference 4.

<sup>e</sup>Reference 5.

<sup>f</sup>Reference 20.

<sup>g</sup>Reference 21.

the line from  $\Gamma$  to  $A$ , and has a large anharmonicity and a large electron-phonon coupling. Anharmonicity increases the frequency by 20% and weakens the corresponding electron-phonon couplings by 30%. The calculated anharmonic frequency, 75.9 meV, for the  $E_{2g}$  mode at  $\Gamma$ , agrees very well with the results from Raman measurements [75.9 meV (Ref. 20) and 76.9 meV (Ref. 21)] as well as other theoretical calculations.<sup>15,16</sup> The  $E_{2g}$  modes at  $M$ ,  $L$ ,  $K$ , and  $H$ , however, have very little anharmonicity and small electron-phonon coupling. The strong anharmonicity and the large electron-phonon coupling are thus confined to phonons in a small volume in  $k$  space near the  $\Gamma$  to  $A$  line.

The calculated phonon frequencies and electron-phonon matrix elements  $g_{\vec{k},\vec{k}'}^j = \langle \vec{k} | \delta V_q^j | \vec{k}' \rangle$  for the  $j$ th phonon mode are interpolated onto a  $18 \times 18 \times 12$  grid in the BZ through the following three-step process. First, we interpolate the dynamical matrices using a weighted average of those at the symmetry points and obtain the phonon frequencies and eigenvectors on the grid by diagonalizing the dynamical matrices. Second, we interpolate the induced crystal potential change by a phonon on the grid from the calculated crystal potential changes at the symmetry points using weighting factors determined from the phonon frequencies and polarization vectors calculated on the fine grid. Finally, we calculate the electron-phonon matrix elements on the grid using the interpolated crystal potential change. All calculations are done twice for comparison: one with harmonic phonon frequencies and another with anharmonic phonon frequencies. To study the isotope effect, we repeat the entire procedure with an isotopic atomic mass.

Figure 1 shows the phonon density of states  $F(\omega)$  and the standard Eliashberg function  $\alpha^2F(\omega)$ . The phonon density of states shows a large peak at 37 meV arising from the Van Hove singularities in the acoustic phonons, but these phonons make no significant contribution to  $\alpha^2F(\omega)$ . There is a large dominant peak in  $\alpha^2F(\omega)$  at 63 meV for the case of harmonic phonons but at 77 meV for anharmonic phonons. The dominant peak in  $\alpha^2F(\omega)$  is caused by the in-plane B–B stretching modes ( $E_{2g}$ ). Because the  $E_{2g}$  modes are highly anharmonic and have very large electron-

phonon coupling only for phonons within a small volume along the  $\Gamma$  to  $A$  line in  $k$  space, anharmonicity has little effect on  $F(\omega)$ , but it causes a big shift in  $\alpha^2F(\omega)$ . In the case of harmonic phonons, as is shown in Table I, the isotropic average electron-phonon coupling constant,  $\lambda = 2 \int d\omega \alpha^2 F(\omega) / \omega$ , is 0.73 and the logarithmic average frequency,  $\omega_{ln} = \exp[(2/\lambda) \int d\omega \alpha^2 F(\omega) \ln \omega / \omega]$ , is 59.4 meV. These values and the overall shape of  $\alpha^2F(\omega)$  without anharmonicity in the present calculation are in good agreement with previous calculations.<sup>14,16</sup> With anharmonicity,  $\lambda$  is reduced to 0.61 and  $\omega_{ln}$  is increased to 63.5 meV. Since  $\lambda$  corresponds to the mass enhancement factor for the density of states at the Fermi level regardless of anisotropy in the electron-phonon interaction,<sup>22</sup> we can compare the calculated  $\lambda$  with results of specific-heat measurements. The reduced value of  $\lambda = 0.61$  due to anharmonicity agrees very well with result of specific-heat measurements which give a  $\lambda$  of 0.58 (Ref. 4) and 0.62.<sup>5</sup> This agreement is evidence that phonon anharmonicity weakens the electron-phonon interaction in MgB<sub>2</sub>. However if this value of  $\lambda = 0.61$  is used in the McMillan<sup>23</sup> or the Allen-Dynes<sup>24</sup> formula for  $T_c$ , the predicted  $T_c$  would be far lower than experiment.

Unlike previous studies, we solve the fully anisotropic

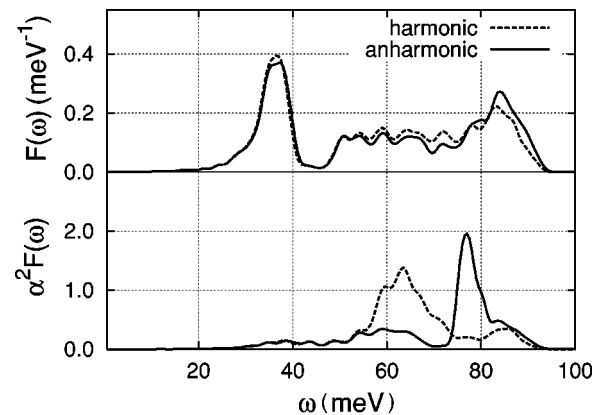


FIG. 1. Phonon density of states  $F(\omega)$  and the isotropic Eliashberg function  $\alpha^2F(\omega)$  for MgB<sub>2</sub>.

Eliashberg equation for superconductivity in MgB<sub>2</sub>. The anisotropic Eliashberg equation at  $T_c$  (Ref. 22) is

$$Z(\vec{k}, i\omega_n) = 1 + f_n s_n \sum_{\vec{k}' n'} W_{\vec{k}'} \lambda(\vec{k}, \vec{k}', n - n') s_{n'},$$

$$Z(\vec{k}, i\omega_n) \Delta(\vec{k}, i\omega_n) = \sum_{\vec{k}' n'} W_{\vec{k}'} f_{n'} [\lambda(\vec{k}, \vec{k}', n - n') - \mu^*(\omega_c)] \times \Delta(\vec{k}', i\omega_{n'}), \quad (1)$$

where  $\omega_n = (2n + 1)\pi T_c$ ,  $f_n = 1/|2n + 1|$ , and  $W_{\vec{k}}$  is the fraction of the density of states at  $\vec{k}$  on the Fermi surface. The cutoff frequency  $\omega_c$  is set to 0.5 eV which is about six times larger than the maximal phonon frequency. For the definition of  $Z$ ,  $\Delta$ ,  $\lambda(\vec{k}, \vec{k}', n)$ , and  $s_n$ , see Ref. 22. With the exception of  $\mu^*(\omega_c)$ , our calculation of the phonon frequencies and electron-phonon interaction provides all the material parameters for solving Eq. (1) and hence for obtaining  $T_c$  from first principles. The dimensionless Coulomb pseudopotential  $\mu^*(\omega)$ , which is defined by  $\mu^*(\omega) = \mu/[1 + \mu \ln(\epsilon_F/\omega)]$ , is known to be of order 0.1 in most metals when  $\omega$  is a relevant phonon frequency,<sup>23,25,26</sup> and we show below that the superconducting properties of MgB<sub>2</sub> are not very sensitive to  $\mu^*(\omega_c)$ . For comparison, we also calculate  $T_c$  using the isotropic Eliashberg equation,

$$Z(i\omega_n) = 1 + f_n s_n \sum_{n'} \lambda(n - n') s_{n'},$$

$$Z(i\omega_n) \Delta(i\omega_n) = \sum_{n'} f_{n'} [\lambda(n - n') - \mu^*(\omega_c)] \Delta(i\omega_{n'}), \quad (2)$$

where  $\lambda(n) \equiv \sum_{\vec{k}\vec{k}'} W_{\vec{k}} W_{\vec{k}'} \lambda(\vec{k}, \vec{k}', n)$ . Hence  $\lambda(n)$  is the electron-phonon coupling averaged over all pairs of  $(\vec{k}, \vec{k}')$  on the Fermi surface. [ $\lambda(n=0)$  is equal to the specific heat  $\lambda$  discussed above.] The isotropic Eliashberg equation is thus a special limited case of the more general anisotropic equation. If the electron-phonon interaction  $\lambda(\vec{k}, \vec{k}', n)$  did not depend strongly on the electronic states on the Fermi surface, the isotropic equation would be an appropriate approximation.

Figure 2 shows the variation of the calculated electron-phonon interaction on the Fermi surface of MgB<sub>2</sub>. The Fermi surface of MgB<sub>2</sub> consists of four sheets; two holelike coaxial cylinders consisting of  $\sigma$ -boron in-plane states along  $\Gamma$  to A, a holelike tubular network of  $\pi$ -boron states connecting regions near K and M, and an electronlike tubular network of  $\pi$ -boron states connecting regions near H and L. In Fig. 2, the mass enhancement factor for states at  $\vec{k}$  given by  $\lambda(\vec{k}, n=0) = \sum_{\vec{k}'} W_{\vec{k}'} \lambda(\vec{k}, \vec{k}', n=0)$  shows two well-separated sets of values on the Fermi surface.  $\lambda(\vec{k}, n=0)$  is about 0.8–1.0 on the two  $\sigma$  cylindrical sheets and is only about 0.3–0.5 on the two  $\pi$  sheets. For more detail, we depict the value of  $\lambda(\vec{k}=\vec{k}_0, \vec{k}', n=0)$  as a function of  $\vec{k}'$  for a fixed  $\vec{k}=\vec{k}_0$  on the Fermi surface near  $\Gamma$ . It shows strong and varying

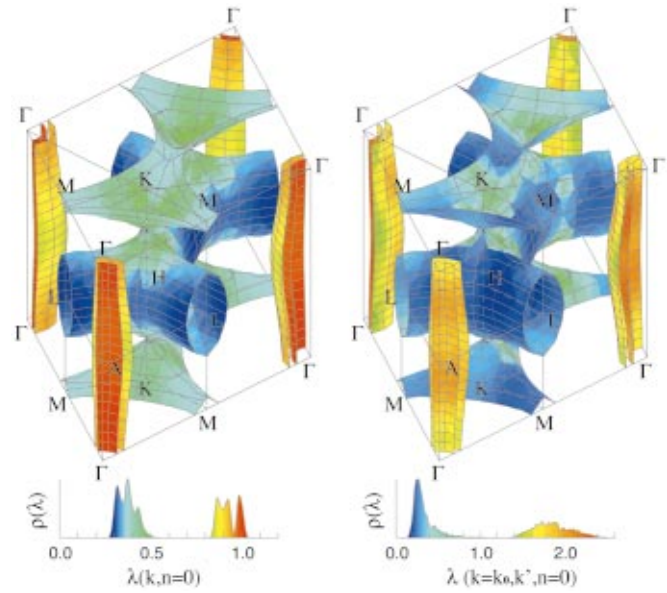


FIG. 2. (Color) Variation of the electron-phonon interaction  $\lambda$  on the Fermi surface of MgB<sub>2</sub>. The left plot shows the mass enhancement factor given by  $\lambda(\vec{k}, n=0)$ . The right plot shows  $\lambda(\vec{k}=\vec{k}_0, \vec{k}', n=0)$  as a function of  $\vec{k}'$  for a fixed  $\vec{k}_0$  on the Fermi surface near  $\Gamma$ .

strength for scattering onto the  $\sigma$  cylindrical surfaces but rather weak strength for scattering to the  $\pi$  sheets. Figure 3 shows the number density of  $(\vec{k}, \vec{k}')$  pairs on the Fermi surface plotted as a function of the value of  $\lambda(\vec{k}, \vec{k}', n=0)$ . The coupling strength  $\lambda(\vec{k}, \vec{k}', n=0)$  between states on the  $\sigma$  cylindrical sheets has values exceeding 2.0 which is much larger than those within the  $\pi$  tubular sheets or between a  $\sigma$  cylindrical sheet and a  $\pi$  tubular sheet. All this information and  $\lambda(\vec{k}, \vec{k}', n)$  with nonzero  $n$  are taken into account when solving the anisotropic Eliashberg equation.

The anisotropic Eliashberg equation including anharmonicity in the phonon frequencies yields  $42 \text{ K} \geq T_c \geq 37 \text{ K}$

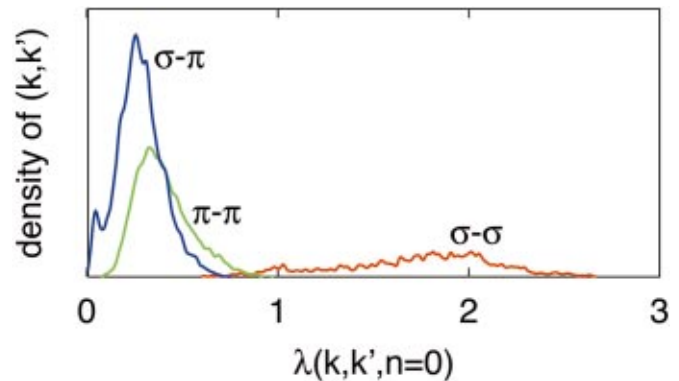


FIG. 3. (Color) Number density of  $(k, k')$  pairs on the Fermi surface versus the value of  $\lambda(\vec{k}, \vec{k}', n=0)$ . The number density is split into three sets: both  $k$  and  $k'$  are on the two  $\sigma$  cylindrical sheets of the Fermi surface (red line), both on the two  $\pi$  tubular sheets (green line), and one on a  $\sigma$  cylindrical sheet and the other on a  $\pi$  tubular sheet (blue line).

for  $0.10 \leq \mu^*(\omega_c) \leq 0.14$ . In particular,  $T_c$  is 39 K when  $\mu^*(\omega_c) = 0.12$ , which corresponds to  $\mu^*(\omega_{\text{in}}) = 0.10$ . To investigate the role of anisotropy in the electron-phonon interaction and of anharmonicity of the phonons, we calculate  $T_c$  disregarding one or the other, as shown in Table I. If we neglect the anisotropy and calculate  $T_c$  with the isotropic Eliashberg equation,  $T_c$  drops to 19 K for  $\mu^*(\omega_c) = 0.12$ . This shows that the strong variation in the electron-phonon coupling of scattering on the Fermi surface is crucial to the observed high  $T_c$  in  $\text{MgB}_2$ . As another comparison, if we calculate  $T_c$  using the anisotropic Eliashberg equation but neglect the anharmonic effect in the phonon frequencies,  $T_c$  goes up to 55 K for  $\mu^*(\omega_c) = 0.12$ . Hence anharmonicity lowers  $T_c$  in  $\text{MgB}_2$ . Thus we conclude that anisotropy in  $\text{MgB}_2$  is essential to produce the anomalously high  $T_c$ , especially in view of the fact that the electron-phonon interaction is weakened by anharmonicity. We note that in  $\text{MgB}_2$ , an average electron-phonon coupling  $\lambda$  cannot be correctly determined from  $T_c$  using the McMillan<sup>23</sup> or Allen-Dynes<sup>24</sup> equations. However, a determination of  $\lambda$  from the specific-heat measurement is still valid. The  $T_c$  of  $\text{MgB}_2$  is not a function of the usual isotropically averaged electron-phonon interaction  $\lambda$  given above; it depends on the details of electron-phonon interaction on the full Fermi surface. This explains the apparent discrepancy between the values of  $\lambda$  estimated from specific-heat measurements and  $\lambda$  estimated from  $T_c$  using simplified isotropic models.

To calculate the isotope-effect exponent  $\alpha$  ( $T_c \propto M^{-\alpha}$ ), we recalculate  $T_c$  using the mass of either  $^{10}\text{B}$  or  $^{26}\text{Mg}$  in place of the natural atomic weight. In these recalculations, we scale  $\omega_c$  in proportion to  $T_c$  in order to avoid a discrete change of the number  $N$  of  $\omega_n$ 's in Eq. (1) [or Eq. (2)]. A change of  $N$  may introduce slight numerical errors in analyzing a small change in  $T_c$ . The scaling of  $\omega_c$  causes a change in  $\mu^*(\omega_c)$ , which is simply

$$\delta\mu^*(\omega_c) = [\mu^*(\omega_c)]^2 \frac{\delta T_c}{T_c}. \quad (3)$$

Table I shows calculated isotope-effect exponents with

$\mu^*(\omega_c) = 0.12$  both with and without phonon anharmonicity. Without anharmonicity, the slight deviation of the sum of the two exponents,  $\alpha_B$  and  $\alpha_{\text{Mg}}$ , from the value of 1/2 is due to the change of  $\mu^*(\omega_c)$  given by Eq. (3). In contrast, when we include anharmonicity in the phonon frequency, the isotope-effect exponent for boron is substantially suppressed. We obtain  $\alpha_B = 0.32$  and  $\alpha_{\text{Mg}} = 0.03$  from the anisotropic Eliashberg equation with anharmonic phonon frequencies. In this case, the contribution of  $\delta\mu^*(\omega_c)$  to the decrease of  $\alpha_B$  is only 0.01, so the anomalously low isotope-effect exponent is primarily due to phonon anharmonicity.

In conclusion, we have shown from first-principles calculations that  $\text{MgB}_2$  is a conventional phonon-mediated superconductor whose properties require, for a correct description, a solution of the fully anisotropic Eliashberg equation including phonon anharmonicity. The isotropic Eliashberg equation seriously underestimates  $T_c$  because it fails to account for the  $(\vec{k}, \vec{k}')$  dependency of the electron-phonon interaction on the Fermi surface. We show that the electron-phonon coupling is exceedingly strong for certain pairs of  $(\vec{k}, \vec{k}')$  on the disconnected Fermi surface of this material. The anisotropy of the electron-phonon interaction in  $\text{MgB}_2$  is strong enough to produce the observed  $T_c$  of 39 K in spite of a moderate average electron-phonon interaction as also seen in specific-heat measurements. In addition, we have shown that the anharmonicity of the phonons in  $\text{MgB}_2$  weakens the electron-phonon interaction and reduces the boron isotope-effect exponent.

This work was supported by National Science Foundation Grant No. DMR00-87088, and by the Director, Office of Science, Office of Basic Energy Sciences of the U. S. Department of Energy under Contract No. DE-AC03-76SF00098. Computational resources have been provided by the National Science Foundation at the National Center for Supercomputing Applications and by the National Energy Research Scientific Computing Center. H.S. acknowledges financial support from the Berkeley Scholar Program funded by the Tang Family Foundation.

<sup>1</sup>J. Nagamatsu *et al.*, Nature (London) **410**, 63 (2001).

<sup>2</sup>S.L. Bud'ko *et al.*, Phys. Rev. Lett. **86**, 1877 (2001).

<sup>3</sup>D.G. Hinks *et al.*, Nature (London) **411**, 457 (2001).

<sup>4</sup>Y. Wang *et al.*, Physica C **355**, 179 (2001).

<sup>5</sup>F. Bouquet *et al.*, Phys. Rev. Lett. **87**, 047001 (2001).

<sup>6</sup>F. Bouquet *et al.*, Europhys. Lett. **56**, 856 (2001).

<sup>7</sup>H.D. Yang *et al.*, Phys. Rev. Lett. **87**, 167003 (2001).

<sup>8</sup>F. Giubileo *et al.*, Phys. Rev. Lett. **87**, 177008 (2001).

<sup>9</sup>S. Tsuda *et al.*, Phys. Rev. Lett. **87**, 177006 (2001).

<sup>10</sup>P. Szabó *et al.*, Phys. Rev. Lett. **87**, 137005 (2001).

<sup>11</sup>F. Laube *et al.*, cond-mat/0106407 (unpublished).

<sup>12</sup>J. Kortus *et al.*, Phys. Rev. Lett. **86**, 4656 (2001).

<sup>13</sup>J.M. An and W.E. Pickett, Phys. Rev. Lett. **86**, 4366 (2001).

<sup>14</sup>K.-P. Bohnen *et al.*, Phys. Rev. Lett. **86**, 5771 (2001).

<sup>15</sup>T. Yildirim *et al.*, Phys. Rev. Lett. **87**, 037001 (2001).

<sup>16</sup>A.Y. Liu *et al.*, Phys. Rev. Lett. **87**, 087005 (2001).

<sup>17</sup>Y. Kong *et al.*, Phys. Rev. B **64**, 020501 (2001).

<sup>18</sup>S.V. Shulga *et al.*, cond-mat/0103154 (unpublished).

<sup>19</sup>H.J. Choi, D. Roundy, H. Sun, M.L. Cohen, and S.G. Louie, Nature (London) (to be published).

<sup>20</sup>J. Hlinka *et al.*, Phys. Rev. B **64**, 140503 (2001).

<sup>21</sup>A.F. Goncharov *et al.*, Phys. Rev. B **64**, 100509 (2001).

<sup>22</sup>P.B. Allen and B. Mitrović, in *Solid State Physics*, edited by H. Ehrenreich, F. Seitz, and D. Turnbull (Academic, New York, 1982), Vol. 37, p. 1, and references therein.

<sup>23</sup>W.L. McMillan, Phys. Rev. **167**, 331 (1968), and references therein.

<sup>24</sup>P.B. Allen and R.C. Dynes, Phys. Rev. B **12**, 905 (1975).

<sup>25</sup>P. Morel and P.W. Anderson, Phys. Rev. **125**, 1263 (1962).

<sup>26</sup>J.P. Carbotte, Rev. Mod. Phys. **62**, 1027 (1990).